OFFICE OF NAVAL RESEARCH

Grant #N00014-91-J-1630
R&T Code 313s002---05

Technical Report #20

Linear and Nonlinear Spectroscopy With the Tunable AC Scanning Tunneling Microscope

by

S. J. Stranick, L. A. Bumm, M. M. Kamna and P. S. Weiss

Department of Chemistry
152 Davey Laboratory
The Pennsylvania State University
University Park, PA 16802

Prepared for publication in

Photons and Local Probes

10 October 1994

REPORT DOCUMENTATION PAGE

Form Approved
OMB No. 0704-0188

1. AGENCY USE ONLY (Leave blank)	2. REPORT DATE	3. REPORT TYPE AND DATES COVERED
	10 October 1994	Technical 6/1/94–5/31/95

4. TITLE AND SUBTITLE
Linear and Nonlinear Spectroscopy With the Tunable AC Scanning Tunneling Microscope

5. FUNDING NUMBERS
N00014-91-J-1630

6. AUTHOR(S)
S. J. Stranick, L. A. Bumm, M. M. Kamna, and P. S. Weiss

7. PERFORMING ORGANIZATION NAME(S) AND ADDRESS(ES)
Department of Chemistry
152 Davey Laboratory
The Pennsylvania State University
University Park, PA 16802

8. PERFORMING ORGANIZATION REPORT NUMBER
Report #20

9. SPONSORING / MONITORING AGENCY NAME(S) AND ADDRESS(ES)
Office of Naval Research
Chemistry Program
800 N. Quincy Street
Alexandria, VA 22217-5000

10. SPONSORING / MONITORING AGENCY REPORT NUMBER

11. SUPPLEMENTARY NOTES
Prepared for publication in *Photons and Local Probes*

12a. DISTRIBUTION / AVAILABILITY STATEMENT
Approved for public release.
Distribution unlimited.

12b. DISTRIBUTION CODE

13. ABSTRACT (Maximum 200 words)

The tunable microwave frequency AC scanning tunneling microscope (ACSTM) has opened the possibility of recording local spectra and local chemical information on insulator surfaces much as the conventional STM has done for metals and semiconductors. We describe the various types of spectroscopies that can be performed with the ACSTM. These include linear spectroscopies where the amplitude at the modulation frequency is measured as well as nonlinear spectroscopies utilizing the amplitudes of the harmonics of the modulation frequency generated in the tunneling junction. Spectrosocpy in the microwave frequency range also enables heretofore unrealizable measurements on conducting substrates such as the rotational spectroscopy of a single adsorbed molecule.

14. SUBJECT TERMS	15. NUMBER OF PAGES	16. PRICE CODE
	13 pages	

17. SECURITY CLASSIFICATION OF REPORT	18. SECURITY CLASSIFICATION OF THIS PAGE	19. SECURITY CLASSIFICATION OF ABSTRACT	20. LIMITATION OF ABSTRACT
Unclassified	Unclassified	Unclassified	UL

LINEAR AND NONLINEAR SPECTROSCOPY WITH THE TUNABLE AC SCANNING TUNNELING MICROSCOPE

S. J. STRANICK, L. A. BUMM, M. M. KAMNA, and P. S. WEISS*
Department of Chemistry
152 Davey Laboratory
The Pennsylvania State University
University Park, PA 16802-6300
USA

Abstract

The tunable microwave frequency AC scanning tunneling microscope (ACSTM) has opened the possibility of recording local spectra and local chemical information on insulator surfaces much as the conventional STM has done for metals and semiconductors. We describe the various types of spectroscopies that can be performed with the ACSTM. These include linear spectroscopies where the amplitude at the modulation frequency is measured as well as nonlinear spectroscopies utilizing the amplitudes of the harmonics of the modulation frequency generated in the tunneling junction. Spectroscopy in the microwave frequency range also enables heretofore unrealizable measurements on conducting substrates such as the rotational spectroscopy of a single adsorbed molecule.

1. Introduction

The scanning tunneling microscope (STM) has enabled a host of measurements of local chemical environment on metal and semiconductor surfaces [1–3]. Related techniques have sprung up which have allowed imaging of insulator surfaces [4,5]. Recent advances in near-field microscopies have enabled the spectra and dynamics of single molecules on surfaces to be recorded under special circumstances, but the imaging resolution remains in the 10 nm range under optimal conditions [6–9].

A number of AC scanning tunneling microscopes have now been put together since Kochanski's initial invention of the technique [10–15]. The exciting possibility of these instruments is that one may combine the consistent atomic resolution of the STM with spectroscopic capabilities on surfaces with arbitrary electronic properties including insulators [16,17]. As described in this paper, a variety of spectroscopic measurements can be performed with these instruments.

---

*Author to whom correspondence should be addressed. E-mail: stm@psuvm.psu.edu.

To appear in
Photons and Local Probes
O. Marti and R. Möller, eds. (Kluwer, 1995)

2. Experimental

The experiments described here were conducted in specially designed scanning tunneling microscopes equipped to handle microwave frequency signals up to 20 GHz. These various ACSTMs have been described previously [13–15]. We have operated ACSTMs both under ambient conditions and in ultrahigh vacuum (UHV) [13–15]. Importantly, for

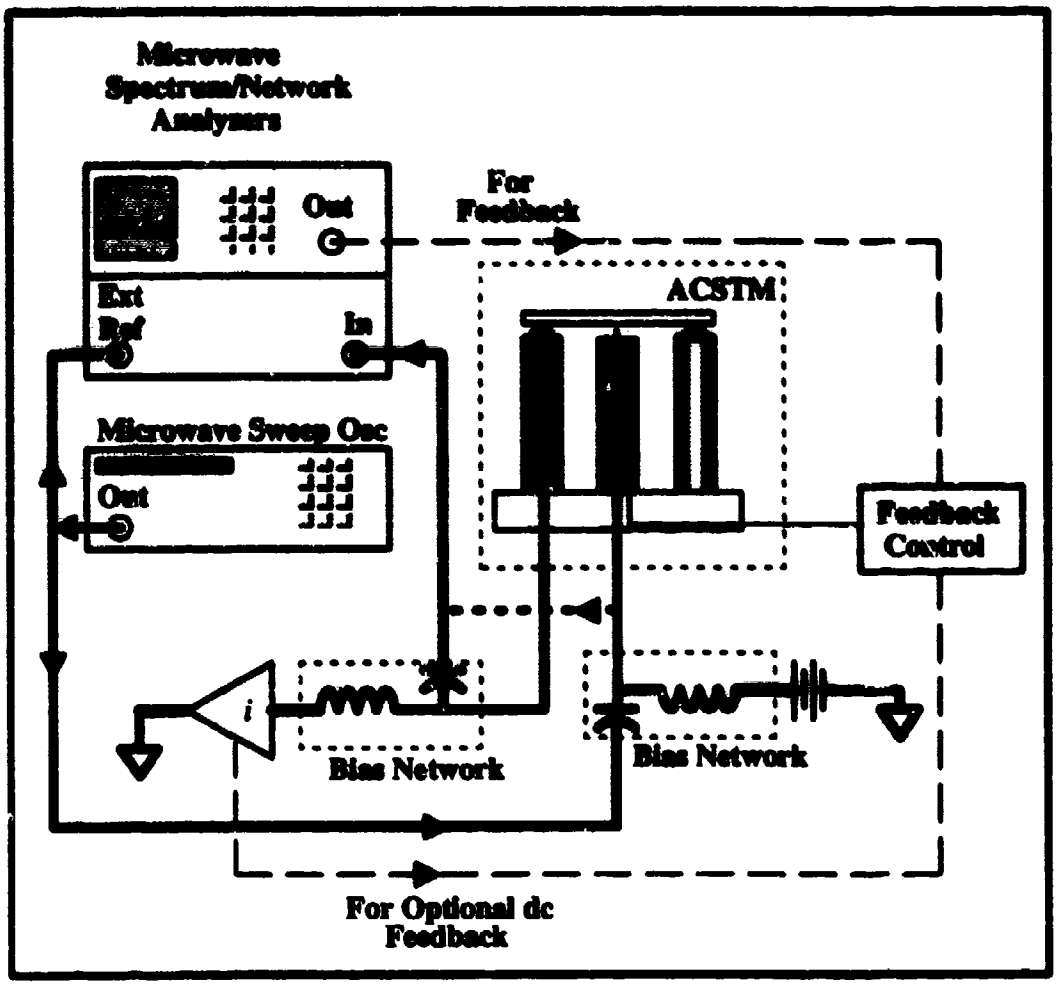

Figure 1. Schematic of the tunable ACSTM signal and control electronics. A microwave sweep oscillator supplies the ACSTM tip with the microwave frequency AC bias. Using a bias network a DC offset can also be applied. The reflected and/or transmitted microwaves are measured using network or spectrum analyzers. Feedback control of the probe tip can be accomplished using the DC current as in conventional STM or using the AC signal at the modulation frequency or one of its harmonics.

understanding the spectroscopy of adsorbates on surfaces, we can operate the UHV ACSTMs at temperatures as low as 4K [15]. We briefly review the critical components of our tunable ACSTMs. We also discuss a recent advance which has resulted in a lower and flatter background for spectroscopic measurements with the ACSTM [18].

A schematic of the instrument and detection scheme is shown in Figure 1 above. A narrow band microwave frequency oscillator is used to supply the microwave frequency modulation to the ACSTM probe tip. The oscillator has a bandwidth of 1 Hz and is tunable over the range 10 MHz–20 Ghz [19]. For sufficiently conducting samples, we use a bias network to supply a dc bias to the ACSTM probe tip along with the microwave frequency modulation and to separate the microwave and low frequency components of the tunneling current [20]. In this way, conventional STM can be used to provide feedback on metal and semiconductor surfaces while microwave signals are simultaneously collected. The small microwave signals are measured using extremely sensitive microwave test equipment [21]. For sufficiently thin insulators, we can record the microwaves transmitted to a conducting backplane. Similarly, we can measure microwave transmission for semiconductors and metals as well. A more general technique particularly useful for studying bulk insulators is to measure the microwaves reflected back down the ACSTM probe tip using a directional coupler or circulator. The signal–to–noise in reflection mode is substantially lower than in transmission mode where both are possible.

The ACSTM head is shown schematically in Figure 2. A beetle–style sample approach is used in all our current instruments [14,15,22]. A microwave frequency coaxial cable is fed through the center (scanner piezoelectric translator tube) [14]. A custom transition is used inside a shielded hypodermic tube within this piezoelectric tube to minimize microwave reflections from within our cabling [18]. For transmission measurements, a second connection is made to another coaxial microwave transmission line through one of the outer walker piezoelectric tubes as indicated in the figure.

Recently, we have found that we can lower and flatten the spectral background of our ACSTM spectra by placing the sample and probe tip in a cavity which is too small to support any resonances within the frequency range of the instrument, 0–22 GHz [18]. The beetle–style sample approach is maintained in this small cavity (diameter ~ 6 mm) by using a liquid metal seal to enclose the tunneling junction electrically [18]. A metal reservoir is attached to the center scanner piezoelectric tube and filled with liquid metal In/Ga/Sn eutectic. A metal insert in the sample holder dips into the liquid metal electrically enclosing the ACSTM tunneling junction. The dimensions of our present small cavity put the lowest supported resonance in the range of 100 GHz, well above any frequency measured in our experiments. This small cavity has the effect that stray reflections of the microwaves off the structures enclosing the ACSTM do not set up standing waves which would interfere with our spectroscopic measurements [18].

Michel and co–workers have come up with an alternate approach for measuring a series of harmonics generated in the ACSTM tunnel junction. They use what is essentially a fixed cavity instrument, but vary the modulation frequency such that the detected harmonic is always at the frequency of the cavity resonance [12,17]. This has the advantage that harmonics can be measured using the impedance match provided by the cavity. The disadvantage is that the harmonic generation can be a function of modulation frequency [16,17]. Nevertheless, with cleverly designed experiments and additional spectroscopic handles, the harmonic spectra obtained can be extremely useful as described below [17].

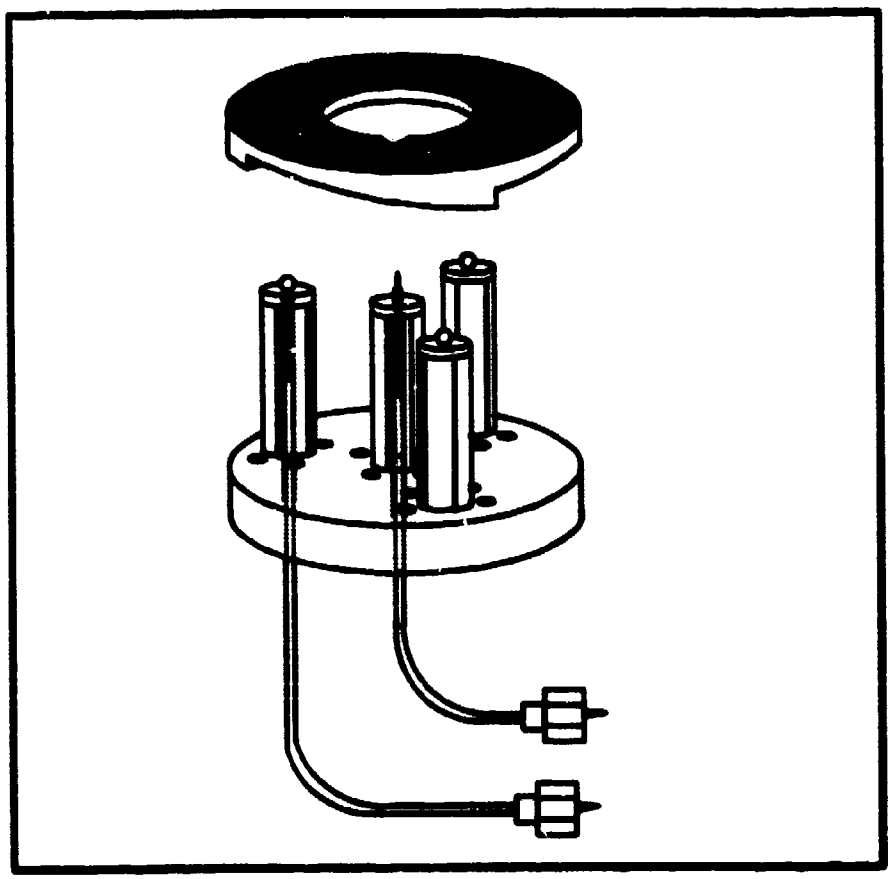

Figure 2. Schematic of the tunable ACSTM head. The microwave frequency bias is supplied by a microwave coaxial cable that runs up the center (scanner) piezoelectric tube. A custom microwave transition is built into a hypodermic tube inside the scanner piezo. Less than 500μ is left unshielded at the end of the probe tip. A beetle style sample approach is used in air and in UHV. For bulk insulators, microwaves reflected back down the probe tip are measured. For conducting samples or thin insulators, transmitted and/or reflected microwaves are used. For transmission AC and for conventional STM measurements, a sample pick-up is used and runs through another of the piezoelectric (walker) tubes.

3. Imaging with the ACSTM

We have been able to achieve atomic resolution on graphite and WSe_2 with microwave frequency feedback mechanisms [16]. On insulating surfaces such as lead silicate glass we have achieved resolution of *ca.* 1 nm [16]. It may be that on crystalline insulators with well-defined stoichiometry, such as the alkali halides, atomic resolution may be routinely obtained, but this remains to be demonstrated. In this regard, the recently constructed UHV ACSTM described above should be of great importance in preparing and in characterizing samples with surface analytical tools prior to imaging.

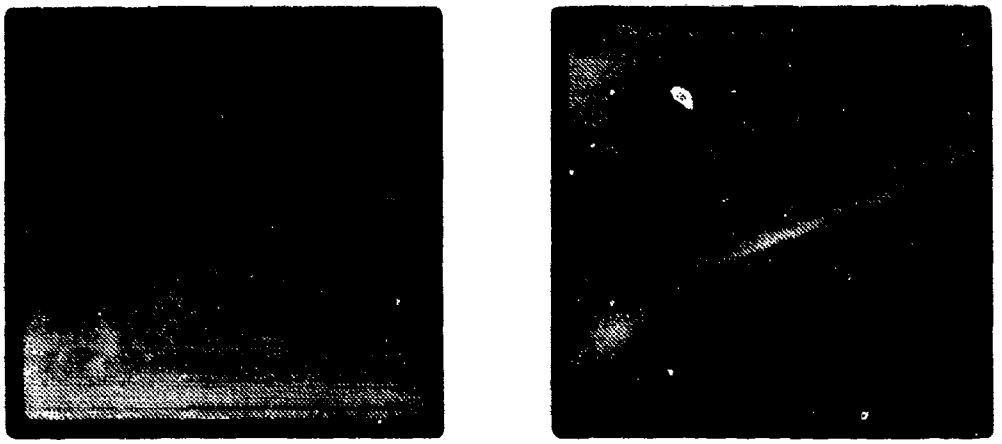

Figure 3. Two images simultaneously recorded of a 1.5μ x 1.5μ region of WSe_2 surface with several multiatomic height steps due to partial exfoliation of the sample. The image on the left shows a constant current conventional STM topograph recorded with V_{tip}=+2.0 V and I_{tunnel}=100 pA. The simultaneously obtained image on the right shows the amplitude at the third harmonic of the AC modulation frequency, f_o=2.440 GHz. Near the exfoliation of the WSe_2 the nonlinearity and thus the third harmonic signal are greatly enhanced. No special features appear in the conventional STM topography in these regions.

By simultaneous imaging in several modes — conventional constant current STM, f_o amplitude, and third harmonic amplitude, for example — we are able to compare features we can readily interpret in topography to the high frequency electronic properties of the surface. Such an experiment is shown in Figure 3. On the left, a conventional STM image shows a region of a WSe_2 surface where the top layers are partially exfoliated at the steps. The simultaneously recorded ACSTM third harmonic signal shows regions adjacent to the exfoliation with greatly enhanced third harmonic signal. We attribute this enhanced nonlinearity to the electronically discontinuous region of the sample. There is greater rectification in these *ca.* 100–200 nm wide regions due to a reduced carrier lifetime compared to the rest of the surface. Michel and co–workers have also adopted this strategy in order to measure doping densities and profiles in Si wafers under a thin oxide layer [17].

One important question to be addressed is the extent to which the microwaves pumped into the tunnel junction heat and/or perturb the adsorbates and surface in the vicinity of the tip. In order to assess the level of this perturbation, we have applied a microwave frequency modulation to the dc bias in conventional low temperature STM measurements of a temperature sensitive sample — benzene on Cu{111} at 77K [15]. A slight increase in temperature would greatly affect the mobility of the benzene molecules which remain fixed at and near steps at this temperature but remain mobile (as a two–dimensional gas) on the Cu{111} terraces [23]. Figure 4 shows a low temperature image of a Cu{111} surface where the benzene molecules adsorbed at the step edges appear unperturbed with microwaves applied to the ACSTM probe tip at 1 GHz. Thus in this case the junction, the sample, and the instrument do not appear to suffer from any deleterious heating effects. We have not seen evidence in any of our experiments for heating of the junction by the microwaves. We note that an additional measurement that can be made is to employ

Figure 4. A conventional STM image of benzene on Cu{111} at 77K in UHV. A microwave modulation at 1 GHz was simultaneously applied to the STM probe tip. The molecules in this regime are extremely sensitive to the substrate temperature. The residence times of the molecules at the various surface sites are not measurably altered with the application of the microwaves indicating that heating of the junction is negligible in this case.

Johnson noise thermometry using frequencies distinct from any supplied to or created (*i.e.* by harmonic generation) in the tunneling junction as in Ref. [24].

4. Spectroscopy with the ACSTM

4.1. LINEAR ACSTM SPECTROSCOPY

Amplitudes of the signal at f_0 and at harmonics, nf_0, can be recorded at a particular position on the surface. This allows us a means to differentiate between the species on the surface, and will ultimately provide spectral handles to identify and to characterize surface species using the ACSTM [16]. The amplitude at f_0 also determines the sensitivity of our instrument at the frequency used for imaging as described in Ref. [13]. We note that dielectric spectra can be assigned in terms of molecular rotations and other motions [16,25]. To this end, we have built a low temperature ultrahigh vacuum ACSTM to measure the rotational spectra of adsorbates in the ACSTM tunnel junction.

Microwave spectroscopy of small molecules in the gas phase has been used to yield structural information [26]. Condensed phase spectra have typically remained uninterpreted. Since molecules are known to perturb the electronic properties of the surrounding surface anisotropically [27], the rotating electronic perturbations of a rotating molecule can be measured at a single surface site as a modulated tunneling current. Since these rotational frequencies are in the microwave to far infrared frequency range, the frequencies at the lower end can be measured in principle with a low temperature ACSTM.

The rotational spectra of adsorbed H_2 molecules on Ag and Cu have previously been measured by electron energy loss spectroscopy [28,29]. Adsorbed PF_3 on a number of

metal surfaces is known from ESDIAD measurements to have a bound (hindered) to free rotor transition as the temperature is increased [30–32]. In NMR experiments, benzene has been shown to rotate on Pt particles which are predominantly textured Pt{111} [33,34]. STM images of azulene have been interpreted as rapidly rotating molecules [35]. We will use benzene molecules to illustrate how we will try to record a rotational spectrum using the ACSTM.

Benzene adsorbed on Pt{111} exhibits three different types of images depending upon adsorption site [27,36]. In the three–fold hollow adsorption sites on the surface, three depressions are seen in the STM images of the surrounding surface. This result is consistent with theoretical calculations of images of benzene and the known variety of binding sites for benzene on Pt{111} [36,37]. Figure 5 shows a schematic of the three lobe image of the benzene molecule and the surrounding surface.

By using conventional (DC) STM feedback and monitoring the AC components of the tunneling current, we expect to be able to measure the rotational frequencies of molecules and to distinguish between bound (frustrated) and free surface rotors. The proposed method for doing this is shown schematically in Figures 5 and 6. The electrons of the substrate, perturbed by the adsorbed molecules would easily follow the motion of the molecules as it rotates. At positions A and B (indicated in Figure 5) for a free rotor, the tunneling current would be modulated at three times the rotation frequency as the (three) apparent depressions of the LDOS are swept past the ACSTM tip by the rotating molecule. Thus the frequency composition at the two probe positions are the same. The frequency spectra are directly related to the rotation frequencies of the molecule. For a frustrated rotor, the molecule twists back and forth in the torsion mode potential well. Even with no excitation there is still zero point motion in this torsion. Once again, the charge follows torsional motion of the molecule. At position A the current is at a maximum when the molecule rotates the apparent depressions in the LDOS away from the probe and is a minimum when the molecule rotate the depressions under the probe tip. Thus the AC

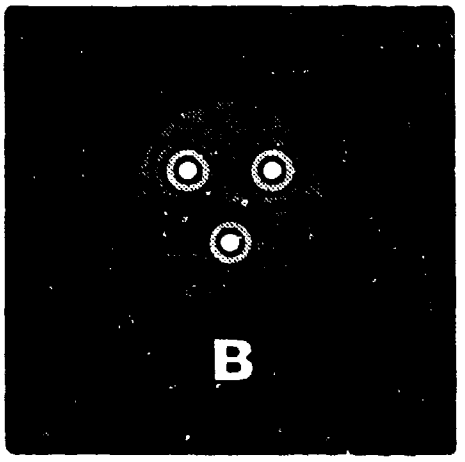

Figure 5. A schematic of a STM image of a benzene molecule in a three–fold hollow site as in Ref. [27] showing three lobes and three depressions in the LDOS of the surrounding substrate. A and B mark the ACSTM probe positions referenced in Figure 6.

component of the current appears at the torsion frequency at position **A**. Position **B** is the center of one of the apparent LDOS depression for the molecule's equilibrium location. Thus in each period, the molecule crosses through the equilibrium position twice. At the equilibrium position, the tunneling current is a minimum. At the maximum excursion from the equilibrium in each direction, the tunneling current is at its maximum. Thus at position **B** the tunneling current would be modulated at twice the torsional frequency by the molecular motion. By noting whether the AC component of the tunneling current varies with position, free and frustrated rotors can then be differentiated. From the frequency spectra of the tunneling current, the rotational/torsional frequencies can be determined. As for gas phase molecules, these frequencies are sensitively dependent on the moments of inertia and thus the structure of the adsorbates. By matching this intramolecular structural information to the local chemical environment measured with the STM, we can probe the modification of intramolecular bonding due to the specific molecular adsorption site.

4.2. NONLINEAR ACSTM SPECTROSCOPY

We have previously discussed how the nonlinear or "harmonic spectra" can be used to glean information as to the local chemical environment by establishing the source(s) of the nonlinearities [16]. Briefly, the tunnel junction non–linearities which lead to harmonic generation are [10,16]:

> *i*) Coulomb blockade effects (where an electron which has just tunneled momentarily repels electrons which otherwise might have tunneled during the same half–cycle, but have insufficient energy) [38],
>
> *ii*) Local density of states which are not constant as a function of energy, and
>
> *iii*) Structural changes (dispersion effects) due to adsorbed or surface layers responding to the ac field.

By having a broadly tunable ACSTM, we are able to tune f_0 and vary its amplitude, and by then also recording amplitudes at a several harmonics, nf_0, we are able to differentiate between these effects. We can thus determine the charging thresholds (*i*), electronic structure (*ii*), and rates of motion (*iii*) of the species on the surface at the position of the ACSTM tip. The nonlinearities above are differentiated based upon their modulation frequency (f_o) and amplitude dependences as follows:

> *i*) Harmonic amplitudes depend on the modulation frequency and amplitude. High harmonic amplitudes simultaneously increase as the modulation amplitude surpasses the (voltage) threshold for tunneling a second electron at the peak of the modulation half–cycle for only a short time [38]. As f_o is reduced and charge can dissipate within a half–cycle, the threshold disappears and the harmonics are reduced.
>
> *ii*) Harmonic amplitudes are frequency independent, but do depend on modulation amplitude.
>
> *iii*) Frequency dependent absorptions and dissipation are characteristic of surface species.

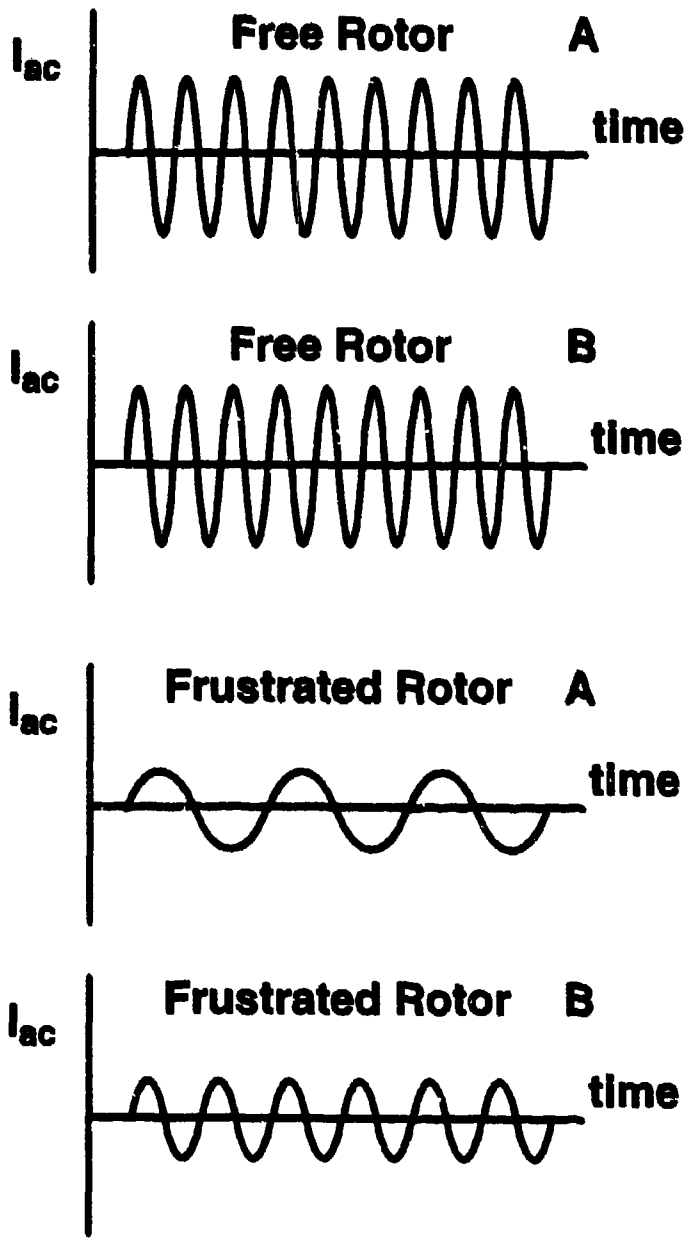

Figure 6. A schematic showing the expected ACSTM current for a free and frustrated rotor when measured at positions A and B shown in Figure 5. For a free rotor the signal is the same for both probe positions and for appears here at three times the rotation frequency. For a frustrated rotor, the signal depends on the probe position. At position A, away from the extremum change in LDOS, the signal appears predominantly at the frustrated rotation frequency. At position B, at the extremum change in LDOS, the signal appears predominantly at twice the frustrated rotation frequency.

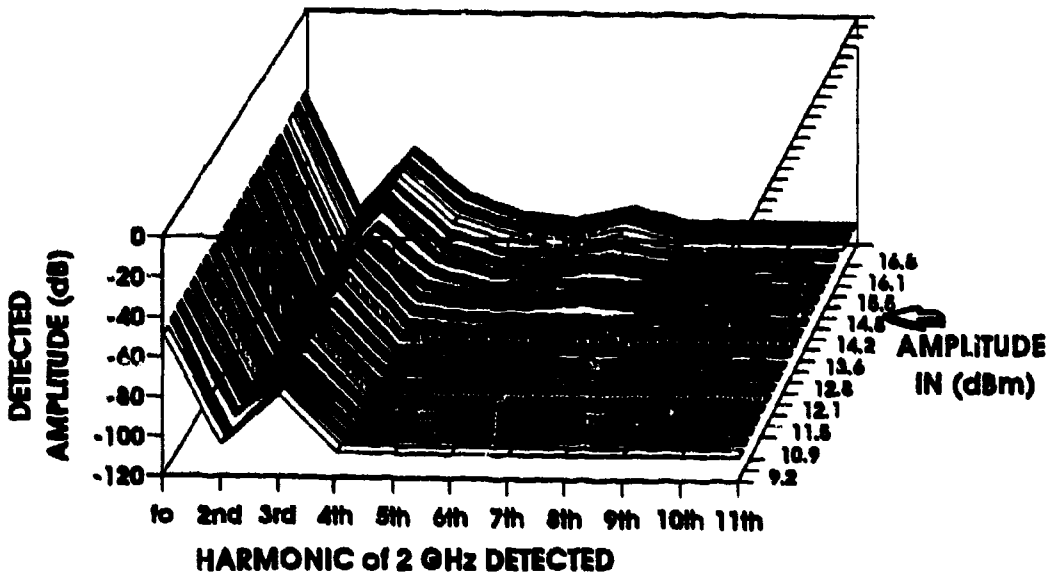

Figure 7. The harmonic amplitudes vary as the modulation amplitude at f_o=2 GHz is changed, and increase sharply as an apparent threshold at 15 dBm (indicated by the arrow) is surpassed.

We previously showed that while probing the same position on a lead silicate glass surface the envelope of harmonics generated in the ACSTM tunneling did depend upon the modulation frequency (for f_o=2.0 and 2.5 GHz) [16]. In Figure 7 we show the dependence of the harmonics generated on the *amplitude* of the modulation applied at f_o=2 GHz. The threshold behavior observed is consistent with a charging effect (*i*). In order to confirm this assignment, we are attempting to measure the charge dissipation rate on the surface by lowering the modulation frequency as described above. We note that it is in only a fraction of the modulation periods that single electrons tunnel [10]. It is then in only a very small fraction of modulation periods in which more than one electron may tunnel; the nonlinearities are not large. It is because we can record over many cycles rapidly using these high modulation frequencies that we are able to measure the nonlinearities due to multiple electron tunneling.

These harmonic measurements enable the identification and study of the species in the tunnel junction in a manner analogous to electrochemical redox measurements and molecular spectroscopy. We now have the means to identify and to characterize the species at the position of the ACSTM tip, and the simultaneous ability to interrogate the chemical environment by imaging the surrounding surface.

5. Prospects

We have shown how the ACSTM can be used to record local chemical and dynamical information on the surfaces of a wide range of materials. This information obtained is complementary to that obtained from conventional STMs and AFMs. By studying well characterized insulator surfaces in UHV, we expect to develop a predictive understanding of the imaging and spectroscopic capabilities of the ACSTM.

Acknowledgments

The authors gratefully acknowledge Kyle Krom for help in the preparation of the figures, Lewis Reynolds for experimental assistance, and helpful discussions with Rick Baer, Steve Clark, Don Coulman, Urs Dürig, Greg Kochanski, Rod Kreuter, Dave Macedonia, Bruno Michel, and Barry Willis. The authors would like to thank the National Science Foundation, the Office of Naval Research, the Biotechnology Research and Development Corporation, and Hewlett–Packard for support of this work.

References

1. Binnig, G. and Rohrer, H. (1982) Scanning Tunneling Microscopy, *Helv. Phys. Acta* **55**, 726–735.
2. Güntherodt, H.–J. and Wiesendanger, R. (1992), *Scanning Tunneling Microscopy I*, Springer–Verlag, New York.
3. Weiss, P. S. (1994), Analytical Applications of Scanning Tunneling Microscopy, *Trends Anal. Chem.* **13**, 61–67.
4. Binnig, G., Quate, C. F., and Gerber, Ch. (1986), Atomic Force Microscope, *Phys. Rev. Lett.* **56**, 930–933.
5. Sarid, D. (1991) *Scanning Force Microscopy: With Applications to Electric, Magnetic and Atomic Forces*, Oxford Univ. Press, Oxford.
6. Betzig, E. and Trautman, J. K. (1993), Near–Field Optics: Microscopy, Spectroscopy, and Surface Modification Beyond the Diffraction Limit, *Science* **257**, 189–195.
7. Betzig, E. and Chichester, R. J. (1993), Single Molecules Observed by Near–Field Scanning Optical Microscopy, *Science* **262**, 1422–1425.
8. Xie, X. S. and Dunn, R. C., Probing Single Molecule Dynamics (1994), *Science* **265**, 361–364.
9. Ambrose, W. P., Goodwin, P. M., Martin, J. C., and Keller, R. A., Alterations of Single Molecule Fluorescence Lifetimes in Near–Field Optical Microscopy (1994), *Science* **265**, 364–367.
10. Kochanski, G. P. (1989), Nonlinear Alternating–Current Tunneling Microscopy, *Phys. Rev. Lett.* **62**, 2285–2288.
11. Siefert, W., Gerner, E., Stachel, M., and Dransfeld, K. (1992), Scanning Tunneling Microscopy at Microwave Frequencies, *Ultramicroscopy* **42–44**, 379–387.
12. Michel, B., Mizutani, W., Schierle, R., Jarosch, A., Knop, W., Benedickter, H., Bächtold, W., and Rohrer, H. (1992), Scanning Surface Harmonic Microscopy: Scanning Probe Microscopy Based on Microwave Field–Induced Harmonic Generation, *Rev. Sci. Instrum.* **63**, 4080–4085.
13. Stranick, S. J. and Weiss, P. S. (1993), A Versatile Microwave Frequency–Compatible Scanning Tunneling Microscope, *Rev. Sci. Inst.* **64**, 1232–1234; *ibid.* **64**, 2039.

14. Stranick, S. J. and Weiss, P. S. (1994), A Tunable Microwave Frequency Alternating Current Scanning Tunneling Microscope, *Rev. Sci. Inst.* **65**, 918–921.
15. Stranick, S. J., Kamna, M. M., and Weiss, P. S. (1994), A Low Temperature, Ultrahigh Vacuum, Microwave–Frequency–Compatible Scanning Tunneling Microscope, *Rev. Sci. Inst.* **65**, in press.
16. Stranick, S. J. and Weiss, P. S. (1994), Alternating Current Scanning Tunneling Microscopy and Nonlinear Spectroscopy, *J. Phys. Chem.* **98**, 1762–1764.
17. Bourgoin, J.–P., Johnson, M. B., and Michel, B. (1994), Semiconductor Characterization with the Scanning Surface Harmonic Microscope, *Appl. Phys. Lett.*, in press.
18. Bumm, L. A. and Weiss, P. S., A Small Cavity Non–Resonant AC Scanning Tunneling Microscope, to be submitted.
19. Hewlett–Packard synthesized sweeper 83620A/008, Hewlett–Packard Co., Palo Alto, CA, USA.
20. Hewlett–Packard high current bias network 11612A/001, Hewlett–Packard Co., Palo Alto, CA, USA.
21. A Hewlett–Packard 8510C/8514B network analyzer is used for phase sensitive detection of the transmitted and reflected signals at the modulation frequency. A Hewlett–Packard 71210C spectrum analyzer is used to record the (scalar) amplitudes at the harmonics of the modulation frequency or to use a particular (*i.e.* third) harmonic for feedback control of the tip height. Hewlett–Packard Co., Palo Alto, CA, USA.
22. Besocke, K. (1987), An Easily Operable Scanning Tunneling Microscope, *Surf. Sci.* **181**, 145–153.
23. Stranick, S. J., Kamna, M. M., and Weiss, P. S. (1994), Atomic Scale Views of a Two–Dimensional Gas–Solid Interface, *Science* **266**, in press.
24. Weiss, P. S. and Eigler, D. M. (1993), What is Underneath? Moving Atoms and Molecules to Find Out, in Vu Thien Binh, N. Garcia and K. Dransfeld (eds.), *Nanosources and Manipulations of Atoms Under High Fields and Temperatures: Applications, NATO ASI Series E: Applied Sciences* **235**, Kluwer Academic, Dordrecht, pp. 213–217.
25. Hedvig, P. (1977), *Dielectric Spectroscopy of Polymers*, Wiley, New York.
26. Townes, C. H. and Schawlow, A. L. (1955), *Microwave Spectroscopy*, McGraw–Hill, New York.
27. Weiss, P. S. and Eigler, D. M. (1993), Site Dependence of the Apparent Shape of a Molecule in STM Images: Benzene on Pt{111}, *Phys. Rev. Lett.* **71**, 3139–3142.
28. Avouris, Ph., Schmeisser, D., and Demuth, J. E. (1982), Observation of Rotational Excitations of H_2 Adsorbed on Ag Surfaces, *Phys. Rev. Lett.* **48**, 199–202.
29. Andersson, S. and Harris, J. (1982), Observation of Rotational Transitions for H_2, D_2, and HD Adsorbed on Cu(100), *Phys. Rev. Lett.* **48**, 545–548.
30. Alvey, M. D. and Yates, Jr., J. T. (1988), Structure and Chemistry of Chemisorbed PF_3, PF_2, and PF on Ni(111): An ESDIAD Study, *J. Am. Chem. Soc.* **110**, 1782–1786.
31. Johnson, A. L., Joyce, S. A., and Madey, T. E. (1988), Electron–Stimulated–Desorption Ion Angular Distributions of Negative Ions, *Phys. Rev. Lett.* **61**, 2578–2581.
32. Joyce, S. A., Johnson, A. L., and Madey, T. E. (1989), Methodology for Electron Stimulated Desorption Ion Angular Distributions of Negative Ions, *J. Vac. Sci. Technol. A* **7**, 2221–2226.
33. Tirendi, C. F., Mills, G. A., Dybowski, C., and Neue, G. (1992), Platinum–Proton Coupling in the NMR Spectrum of Benzene on an Alumina–Supported Catalyst, *J. Phys. Chem.* **96**, 5045–5048.

34. Engelsberg, M., Yannoni, C. S., Jacintha, M. A., and Dybowski, C. (1992), Geometry and Dynamics of Benzene Chemisorbed on a Pt/η–Al_2O_3 Catalyst: A ^{13}C Dipolar NMR Study, *J. Am. Chem. Soc.* **114**, 8319–8320.
35. Hallmark, V. M. and Chiang, S. (1993), Imaging Structural Details in Closely Related Molecular Adsorbate Systems, *Surf. Sci.* **286**, 190–200.
36. Sautet, P. and Bocquet, M.–L. (1994), A Theoretical Analysis of the Site Dependence of the Shape of a Molecule in STM Images, *Surf. Sci. Lett.* **304**, L445–L450; Bocquet, M.–L. (1993), Analyse Théorique d'Images d'Adsorbats Moléculaires Obtenues par Microscopie A Effet Tunnel: Benzène (Isolé) sur Platine(111), Magistère des Sciences de la Matière, Ecole Normale Superieure de Lyon, Lyon, France.
37. Wander, A., Held, G., Hwang, R. Q., Blackman, G. S., Xu, M. L., de Andres, P., Van Hove, M. A., and Somorjai, G. A. (1991), A Diffuse LEED Study of the Adsorption Structure of Disordered Benzene on Pt{111}, *Surf. Sci.* **249**, 21–34.
38. Likharev, K. K. (1988), Correlated Discrete Transfer of Single Electrons in Ultrasmall Tunnel Junctions, *IBM J. Res. Develop.* **32**, 144–158.